Opt Quant Electron (2011) 42:463–472
DOI 10.1007/s11082-010-9429-4

Design of a compact photonic crystal sensor

J. Derbali · F. AbdelMalek · S. S. A. Obayya · H. Bouchriha · R. Letizia

Received: 15 July 2010 / Accepted: 7 December 2010 / Published online: 24 December 2010

Abstract The development of technology in photonic crystal (PC) structures has seen rapid progress. Using PCs in biosensing area may open new venues to achieve single molecule detection, and high resolution scanning. A novel PC sensor with improved performances, in terms of size, compactness and sensitivity is presented in this paper. The sensing element consists of dielectric cylinders with varying radius introduced along <01> and <10> directions of the crystal. The results show that the peak wavelength shifts to the high frequency region when only six cylinders are filled with analytes. Also, the peaks show a larger shift compared to the structure obtained using the entire PC waveguide as sensing region. The proposed sensor shows a better sensitivity to water than other analytes, where the peak wavelength tends to shift towards the low frequency region.

Keywords Photonic crystals · Biosensing · Sensitivity

1 Introduction

Photonic crystals (PCs) are dielectric materials possessing a periodicity in two dimension (2D) or three dimension (3D) directions. By performing a periodic etching of air holes, a photonic band gap can be formed, which allows to manipulate the propagation of the light for a vast number of applications. Amongst all of them, the use of PC technology for sensing applications has recently gained much attention, (Cunin et al. 2002; Block et al. 2006; Sonek

J. Derbali · F. AbdelMalek
National Institute of Applied Sciences and Technology,
BP 676, 1080 Tunis Cedex, Tunisia

S. S. A. Obayya (✉) · R. Letizia
Faculty of Advanced Technology, University of Glamorgan, Pontypridd, UK
e-mail: sobayya@glam.ac.uk

H. Bouchriha
Group of Quantum Physics, Faculty of Sciences of Tunis, Tunis, Tunisia

2005; Akahane et al. 2003; Chow et al. 2004). PCs based optical sensors are believed today to be the key devices for the development of biomedical research, health-care, and medicine (Hasek et al. 2006).

Optical sensors have been a growing and fascinating area, based on two fundamental ways of detecting molecules. The first one is based on the interaction between light and the target molecules, which are labelled with fluorescent tags so that the intensity of fluorescence indicates the presence of the molecules. The second way of detection is label-free and relates the concentration of the molecules to the intensity of fluorescence. The signal from the optical sensor is altered when the target molecules are adsorbed/absorbed in the active region of the sensor. PC based optical sensors measure the changes in the refractive index, which is due to the phenomenon of molecules binding. Developing label-free PCs is crucial to build up portable sensors that are cheap and with small size, hence can provide multiplexed detection capabilities.

PCs biosensors are label-free optical sensors based platforms (Mathias et al. 2007; Lee and Fauchet 2007). Due to their spatial periodicity which is in the order of a wavelength, these structures exhibit a photonic band gap. This band gap depends strongly on the structural parameters of the crystal, such as the refractive indices, the shape of inclusions, and the periodicity. The electromagnetic waves whose wavelength lies within the band gap cannot propagate along the PC. As a result, the transmission spectrum of the photonic crystal shows a band gap whose size matches with that of the photonic band gap. This property is exploited to build waveguides by merely introducing a defect inside the periodic lattice. Breaking the periodicity, for instance by changing either size or refractive index of certain inclusions, corresponds to allowing specific defect propagation modes to appear within the band gap. As a result, the transmission characteristic of the PC structure exhibits a narrow peak within the band gap whose position in frequency relies on the shape, and the size of the defect. When the PC is illuminated with light at same frequency as the defect mode, the source is then allowed to propagate through the crystal while being confined in the defect region. The localized defect mode in the transmission spectrum has the property to be very sensitive to the medium surrounding the defect, and can be used as a sensor to detect the changes in refractive indices. The adsorption of molecules onto the surface of the PC sensor results in the appearance of the sharp peak within the band gap, the higher this is in amplitude the stronger is the interaction between target molecules and light. PC waveguide biosensors have been extensively used to measure refractive index changes of analytes (Topolancik et al. 2003). The modification of the medium properties can be explained by phenomena of molecules binding of target analytes onto the surface of the sensing region within the PC waveguide. Therefore, the variation of the overall effective index alerts the cut-off wavelength shift. Krauss et al. have demonstrated a high sensitivity resulting from the shift of the resonant wavelength peak due to changes in refractive index of chemical involved in a PC cavity (Di Falco et al. 2009).

In this paper, a PC waveguide obtained by introducing line defects in the periodic lattice is optimized for sensing applications. The device operating principle is based on the local change of the refractive index of the defect. Results show that the size of the sensing region can be miniaturized to aid the design of subwave length sensors. The optimum value of the radius of the cylinder is a key parameter to quantify the size of target molecules. This paper is arranged as follows; following this introduction, a brief numerical analysis of the computational method used is presented in Sect. 2. The results and discussions on the proposed sensor device are presented in Sect. 3. Finally conclusions are drawn.

2 Analysis

In order to calculate the band structure we employed the plane expansion method (PWE), the details of the calculations are reported in (Ouerghi et al. 2006).The electromagnetic fields evolution and the transmission spectra are calculated by using the finite difference time domain (FDTD) in Yee scheme (Yee 1966). The electric and magnetic fields are evaluated at different grid points in leapfrog and staggered grid forms. The Maxwell's equations are written as

$$\frac{\partial H_x}{\partial t} = -\frac{1}{\mu}\frac{\partial E_z}{\partial y} \tag{1}$$

$$\frac{\partial H_y}{\partial t} = \frac{1}{\mu}\frac{\partial E_z}{\partial x} \tag{2}$$

$$\frac{\partial E_z}{\partial t} = \frac{1}{\varepsilon}\left(\frac{\partial H_y}{\partial x} - \frac{\partial H_x}{\partial y} - \sigma E_z\right) \tag{3}$$

where, μ is the permeability, ε represents the permittivity and σ is the conductivity.

In this work, we consider the transverse magnetic (TM) polarization, where the magnetic field is normal to the axis of the rods. The magnetic field components Hx and Hy are in the plane (i.e. $Hz = 0$). The computational domain has been discretised using spatial step sizes along x and y direction both equal to $0.025a$, with a representing the lattice constant of the PC, in order to ensure good accuracy of the numerical results (Belhadj et al. 2005). In order to ensure the stability of the FDTD scheme, the spatial and temporal steps are related through the following equation

$$\Delta t = 1 \Big/ \left(c((1/\Delta x)^2 + (1/\Delta y)^2)^{1/2}\right) \tag{4}$$

where c is the speed of light in vacuum, and Δx and Δy are spatial steps in the x- and y-directions, respectively. In order to terminate the computational domain, the perfectly matched layers (PMLs) are employed (Berenger 1994).

3 Results and discussions

The proposed PC sensor consists of a square lattice of air holes drilled on a dielectric of relative permittivity $\varepsilon = 8.9$. The radius of the air hole is $R = 0.2a$, where $a = 380\,\text{nm}$ is the lattice constant. A waveguide is created by substituting lines of air holes along the <10>, and <01> directions with air cylinders of different radius $r = 0.3a$, as shown in Fig. 1a.

Calculating the defect band diagram, a defect mode is identified at normalized frequency $f = 0.3665\ \omega a/2\pi c$ when the polarization of the light is assumed with electric field as perpendicular component to the plane of the structure. The band diagram of the structure when defects are introduced along <01> is reported in Fig. 1b.

In order to investigate the field pattern and spectral response of the proposed sensor, the FDTD method is used. The case of an analyte with refractive index $n = 1.32$ flown the sensing region,along the $<01>$ and $<10>$ direction, is studied first. A continuous wave source at $f = 0.3665\ \omega a/2\pi c$ is injected into the waveguide at the top branch port and let it propagate until the steady state is reached. Due to the symmetry of the structure, for all the cases studied in this paper the top branch is taken as input port, thus a symmetrical response

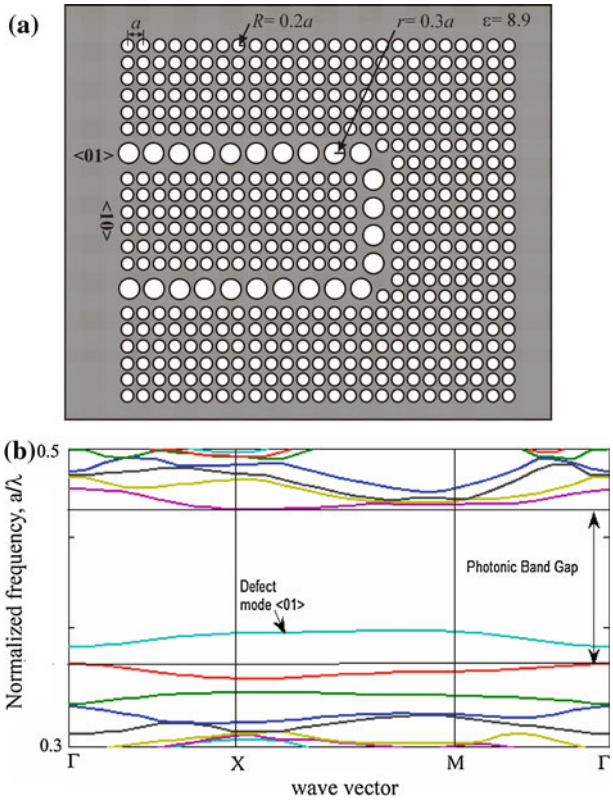

Fig. 1 **a** The photonic structure with line of defects based sensor. **b** Band structure of the PC with defects introduced along <01> direction

of the electric field is assumed if the sensor is excited at the bottom arm. The electric field distribution obtained is shown in Fig. 2a.

It can be observed that the field is strongly confined and propagates along the defect regions with almost constant intensity, thus no significant interaction has occurred between the light, the analyte and the refractive index change has not been relevant. Also, it can be noticed that the field in the lower channel is more intense than that in the upper one. This may be due to the fact that light is tuned resonantly at the corners, which may increase its intensity. Next, the case of an analyte with refractive index $n = 1.33$ is considered. The field distribution reported in Fig. 2b shows that for this case the field intensity along the waveguide varies and it is particularly affected in the <10> direction. This is clearly shown in the upper channel where the field is more intense than its counterpart in the lower one. Also, it can be pointed out that the intensity fluctuates from 0.05 in the lower channel to 0.06 in the upper one.

Also, the interaction between the light and water molecules seems to be stronger compared to the case shown in Fig. 2a. This result can be due to the phenomenon of molecule binding onto the surface of the nanochannel, which results in a perturbation of the effective index. For comparison, the electric field distribution is calculated also for a third case, where the analyte has refractive index $n = 1.34$, as shown in Fig. 2c. From this figure, one may observe that the field is more intense in the upper photonic crystal waveguide than in the lower one. Such

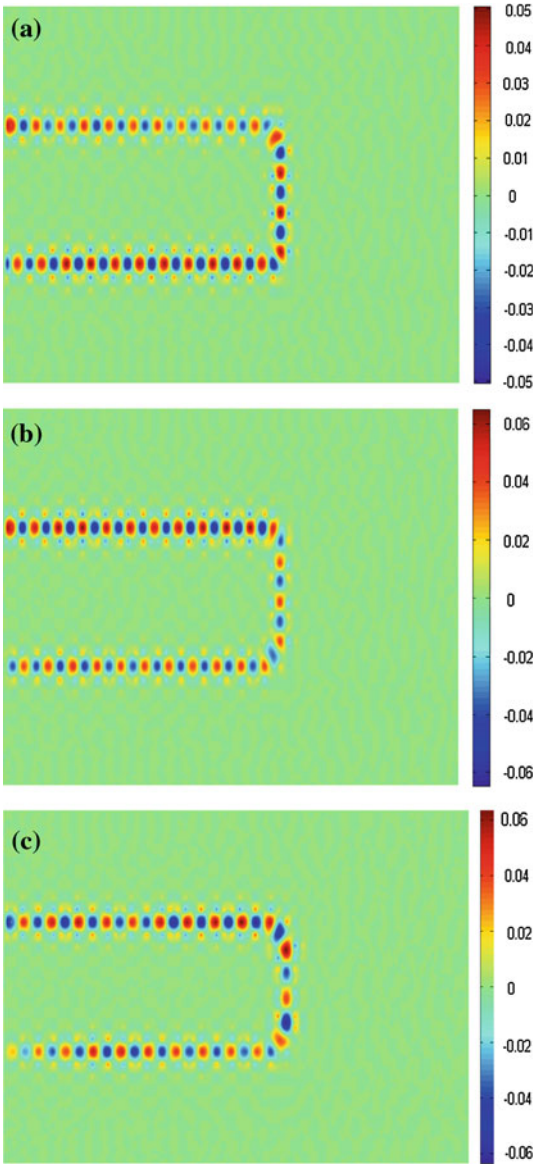

Fig. 2 **a** Electric field distribution at $f = 0.3665\ \omega a/2\pi c$ with $n = 1.32$. **b** Electric field distribution at $f = 0.3665\ \omega a/2\pi c$ when $n = 1.33$. **c** Electric field distribution at $f = 0.3665\ \omega a/2\pi c$ when $n = 1.34$

a situation is similar to the previous case where $n = 1.33$. Therefore, the proposed sensor seems to be more sensitive to water ($n = 1.33$) than the other two analytes with refractive indices $n = 1.32$ and $n = 1.34$.

This may be considered as the first step for the design of a selective biosensor. Next, the transmission characteristic of the waveguide is investigated for the different values of the refractive index n. A Gaussian pulse is injected as source at the input section (top branch) and the time domain variation of the field is recorded at the output of the waveguide (bottom branch). By considering the ratio between the Fast Fourier Transform (FFT) of the time domain data at output and that at input, the transmission spectrum of the structure is

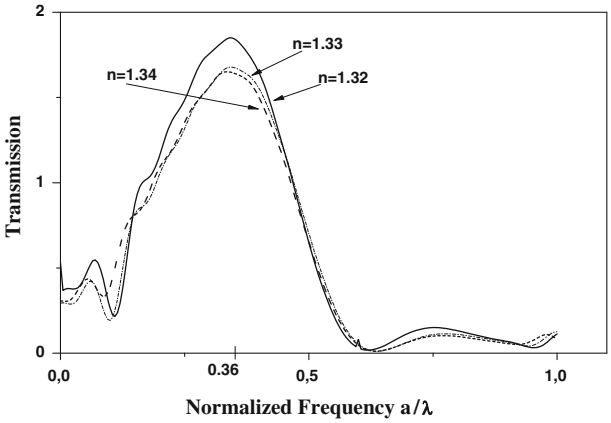

Fig. 3 Transmission versus the normalized frequency for different analytes

calculated as a function of normalized frequency a/λ. Figure 3 shows the results obtained while varying the refractive index from $n = 1.32$ to $n = 1.34$. The transmission peaks observed in this figure represent the resonant wavelength around which the proposed sensor is able to function. It is known that the selectivity of the sensor is based on the phenomena of adsorption/absorption of molecules on the surface, therefore the findings in Fig. 3 suggest that water molecules are adsorbed, leading to a change in the effective index. As a result, the transmission maximum peak shifts.

Based on the results shown in Fig. 2b, it can be understood that the most sensitive region of the structure consists of the line defect along the <10> direction. Therefore, a new design for a miniaturized photonic crystal sensor is proposed by introducing six air cylinders along the <10> direction only. The schematic of the modified structure is shown in Fig. 4a.

In order to determine the frequency of the guided mode, the band structure is calculated and reported in Fig. 4b. The frequency of the guided mode is found to be located at $f = 0.3659\ \omega a/2\pi c$.

In order to optimize the size of the cylinders, the hole radius r is varied whilst the refractive index is kept unchanged and equal to $n = 1.33$. Figure 5 illustrates the transmission spectra obtained in the normalized frequency domain for $r = 0.3a, 0.35a$, and $0.4a$.

From Fig. 5, it can be noted that the curve corresponding to $r = 0.3a$ is narrower compared to the curves obtained for $r = 0.35a$ and $0.4a$. Therefore, cylinders with a radius of $0.3a$ appear to be more suitable to selectively detect analytes. Next, while the cylinders radius is kept fixed at $r = 0.3a$, the refractive index of the analyte filling the cylinders is varied as in previous example in order to understand its effect on the field intensity along the waveguide. For comparison to the previous case, the electric field distribution for the steady-state at $f = 0.3659\ \omega a/2\pi c$ are presented for three different cases in Fig. 6a–c.

From Fig. 6, it can be initially observed that the field intensity in the new sensing region (cylinders introduced along the <10> direction) is different from that shown for the structure in Fig. 1. This is due to the fact that the number of filled cylinders have a large impact on the propagation constant of the electric field. Then, comparing the three cases in Fig. 6 a–c, the reported field profiles do not seem to differ from each other in a significant way. However, the change of refractive index does affect the transmission properties of the structure and this is clearly shown in Fig. 7 where the transmission spectrum of the sensor for the three different

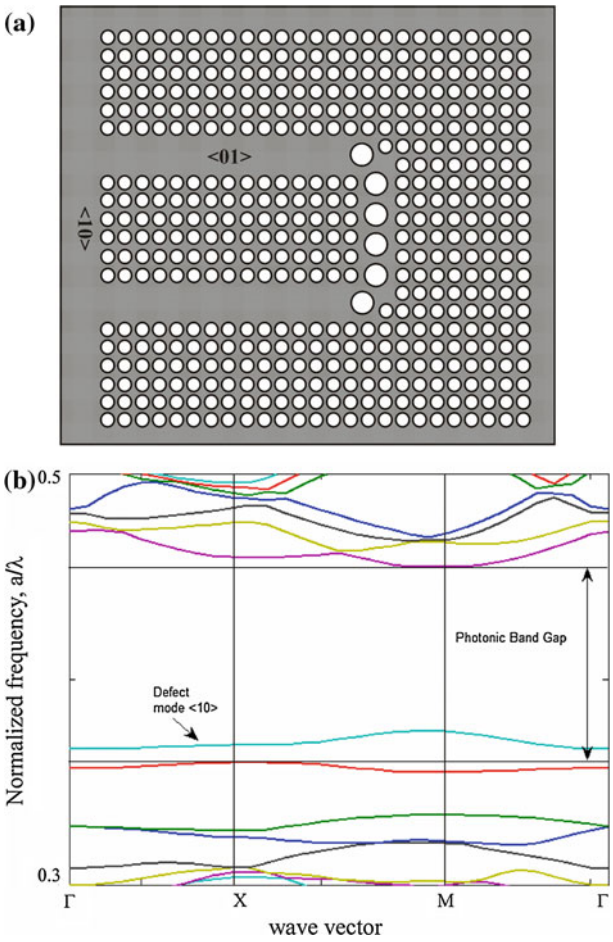

Fig. 4 **a** New design of photonic crystal sensor where the sensing region consists of six cylinders along the <10> direction only. **b** Band structure of the PC with defects introduced along <10> direction

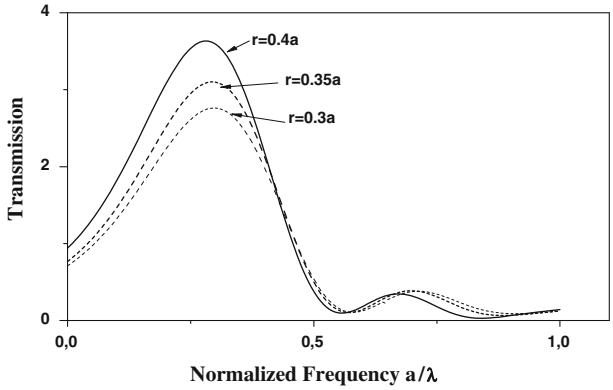

Fig. 5 Transmission versus the normalized frequency with radius of the introduced cylinders equal to $r = 0.3a, 0.35a$, and $0.4a$

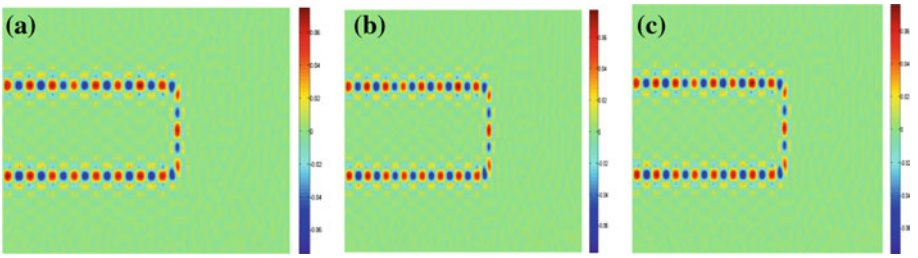

Fig. 6 Snapshot of the electric field at $f = 0.3659\ \omega a/2\pi c$ when $n = 1.32$ (**a**) $n = 1.33$ (**b**), $n = 1.34$ (**c**)

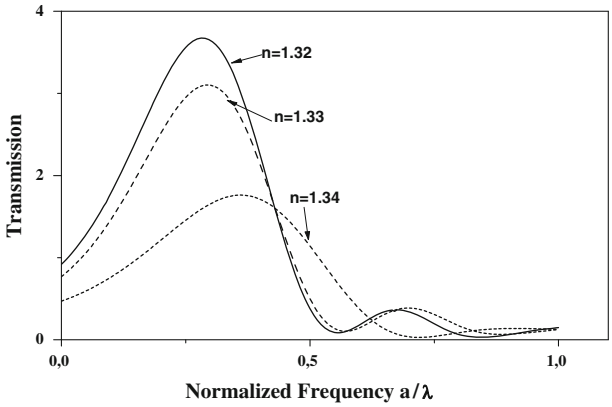

Fig. 7 Transmission variation with the normalized frequency for different values of the refractive index while $r = 0.3a$.

analytes is reported. Comparing Figs. 7 to 3, it can be shown that, although relying of a less number of defect-holes, the sensitivity of the proposed device to the change in the refractive index n is more evident, therefore its response in transmission varies significantly while detecting different analytes. Moreover, the peaks in transmission appear to be less broaden compared to those in Fig. 3. This could be due to the fact that, when the analyte is concentrated in the six cylinders in <10> direction, the field propagating at $f = 0.3659\ \omega a/2\pi c$ finely overlaps the defect mode of the sensing region.This property can contribute in reducing loss noises in the spectrum, however the source bandwidth that can be injected into the device results shortened.

The shift in the peaks of transmission revealed by Fig. 7 is the result of either adsorption or binding of molecules onto the surface.

Next, the sensitivity of the proposed sensor is calculated and reported in Fig. 8. The sensitivity is defined as $s = \Delta\lambda/\Delta n$ where $\Delta\lambda$ represents the distance between the maximum transmission peak for a generic analyte n and that obtained for the case of water, while Δn is the variation of the analyte refractive index from the case of water ($n = 1.33$).From this figure it can be noted that the suggested design is sensitive to water and its sensitivity decreases as Δn increases. Also, the sensitivity decreases rapidly when Δn varies from 0.004 to 0.008. However, this variation in the sensitivity becomes slower for Δn greater than 0.008. In this range the sensor does not seem to be significantly sensitive to analytes. To improve the sensitivity, other parameters such as the surface of the cylinders containing the analytes should be investigated.

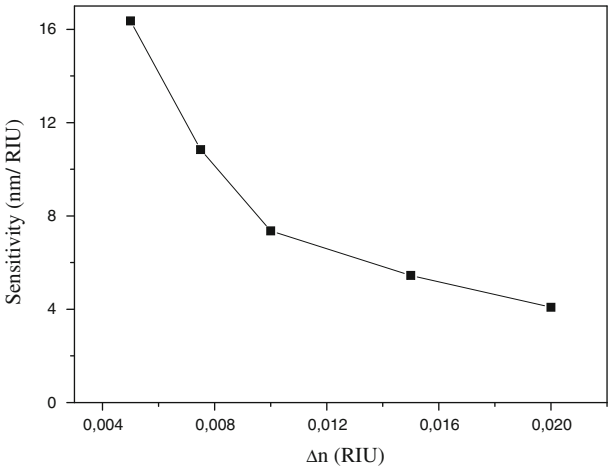

Fig. 8 Sensitivity variation with a change of refractive index Δn from $n = 1.33$.

With reference to Fig. 7, it can be seen that a sensitivity of $s = 1.1$ nm/RIU is obtained when n is varied from 1.32 to 1.33, whereas the sensitivity increases up to $s = 7.36$ nm/RIU when n changes from 1.33 to 1.34.

Compared to other reported photonic crystal-based sensors, the obtained sensitivity can be seen as a reasonable compromise since a reduced interaction length in the sensing region often leads to a deteriorated sensitivity. However, the results presented show that the sensitivity can be significantly improved by optimizing structural parameters of the photonic crystal, such as the radius and the number of the cylinders in the sensing region.In particular, the use of less cylinders to form the sensing region is an important step towards the detection of small molecules and for the design of footprint size sensors.

4 Conclusion

A novel photonic crystal-based sensor with two different sensing area designs has been reported and thoroughly discussed. It has been shown that the sensitivity of the proposed sensor depends mainly on the sensing region structural characteristics. The sensitivity obtained when six cylinders only are considered as a sensing region is higher compared to the sensitivity calculated when the whole nanochannel structure is used as sensing element. Therefore, the simulated results showed that it is possible to reduce the size of the sensing region without affecting its performance. By investigating the transmission spectrum of the sensor, it is also possible to optimize the radius of the cylinders, determining the size of target molecules.

References

Akahane, Y., Asano, T., Song, B., Noda, S.: High-Q photonic nanocavity in a two-dimensional photonic crystal. Nature **425**, 944–947 (2003)

Belhadj, W., Boukari, O., Gamra, D., AbdelMalek, F., Bouchriha, H.: Synthetic Metals, vol. 51, pp. 6–9. (2005)

Berenger, C.J.P.A.: Perfectly matched layer for the absorption of electromagnetic waves. J. Comput. Phys. **114**(2), 185–200 (1994)

Block, I.D., Chan, L.L., Cunningham, B.T.: Photonic crystal optical biosensor incorporating structured low-index porous dielectric. Sens. Actuators B **120**, 187–193 (2006)

Chow, E., Grot, A., Mirkarimi, L.W., Sigalas, M., Girolami, G.: Ultracompact biochemical sensor built with two-dimensional photonic crystal microcavity. Opt. Lett. **29**, 1093–1095 (2004)

Cunin, F., Schmedake, T.A., Link, J.R., Li, Y.Y., Koh, J., Bhatia, S.N., Sailor, M.J.: Biomolecular screening with encoded porous-silicon photonic crystals. Nat. Mater. **1**, 39–41 (2002)

Di Falco, A., O'Faolain, L., Krauss, T.F.: Chemical sensing in slotted photonic crystal heterostructure cavities. Appl. Phys. Lett. **94**, 063503 (2009)

Hasek, T., Wilk, R., Kurt, H., Citrin, D., Koch, M.: Sub-terahertz 2D photonic crystal waveguides for fluid sensing applications. In: Infrared Millimeter Waves and 14th International Conference on Teraherz Electronics, 239 (2006)

Lee, M., Fauchet, P.: Two-dimensional Si photonic crystal microcavity for single particle detection. In: Proceedings of the 4th IEEE International Conference Group IV Photonics IEEE, pp. 1–3. (2007)

Mathias, P.C., Ganesh, N., Chan, L.L., Cunningham, B.T.: Combined enhanced fluorescence and label-free biomolecular detection with a photonic crystal surface. Appl. Opt. **46**, 2351–2360 (2007)

Ouerghi, F., Abdelmalek, F., Haxha, S., Mejatty, M., Bouchriha, H., Haxha, V.: Light confinement in 3D silicon doped with germanium (n-Si_xGe_{1-x}) and silicon-on-insolator (SOI) photonic crystal structures. Opt. Commun. **265**, 683 (2006)

Sonek, G.J.: Integrated photonic crystal waveguides for micro-bioanalytical devices. In: Proceedings of IEEE Conference on Microtechnologies in Medicine and Biology, pp. 333–335. IEEE (2005)

Topolancik, J., Bhattacharya, P., Sabarinathan, J., Yu, P.C.: Fluid detection with photonic crystal-based multichannel waveguides. Appl. Phys. Lett. **82**, 1143–1145 (2003)

Yee, A.S.K.: Numerical solution of initial boundary value problems involving Maxwell's equations in isotropic media. IEEE Trans. Antennas Propag. **AP-14**(4), 302–307 (1966)